Received: 16 November 2019 | Revised: 29 January 2020 | Accepted: 6 February 2020

DOI: 10.1002/bit.27302

ARTICLE

BIOTECHNOLOGY AND BIOENGINEERING WILEY

Detection and destruction of HER2-positive cancer cells by Ultra Quenchbody-siRNA complex

Jinhua Dong[1,2] | Yuya Oka[3] | Hee-Jin Jeong[4] | Yuki Ohmuro-Matsuyama[5] | Hiroshi Ueda[1,5]

[1]Tokyo Tech World Research Hub Initiative, Institute of Innovative Research, Tokyo Institute of Technology, Yokohama, Japan

[2]Key Laboratory of Biological Medicines in Universities of Shandong Province, Weifang Key Laboratory of Antibody Medicines, School of Bioscience and Technology, Weifang Medical University, Shandong, China

[3]Graduate School of Life Science and Technology, Tokyo Institute of Technology, Yokohama, Japan

[4]Department of Biological and Chemical Engineering, College of Science and Technology, Hongik University, Sejong, Korea

[5]Laboratory for Chemistry and Life Science, Institute of Innovative Research, Tokyo Institute of Technology, Yokohama, Japan

Correspondence
Hiroshi Ueda, Laboratory for Chemistry and Life Science, Institute of Innovative Research, Tokyo Institute of Technology, 4259-R1-18 Nagatsuta-cho, Midori-ku, Yokohama 226-8503, Japan.
Email: ueda@res.titech.ac.jp

Funding information
Japan Society for the Promotion of Science, Grant/Award Numbers: JP15H04191, JP18H03851, JP26420793; Natural Science Foundation of Shandong Province, Grant/Award Number: ZR2017MB037; National Natural Science Foundation of China, Grant/Award Number: 21775064

Abstract

Ultra Quenchbody (UQ-body) is a biosensor that utilizes the quenching behavior of the fluorescent dye linked to the antibody V region. When the corresponding antigen is bound to the UQ-body, the fluorescence is restored and allows the detection of target molecules easily and sensitively. In this paper, we constructed UQ-bodies to sensitively detect the human epidermal growth factor receptor 2 (HER2) cancer marker in solution or on cancer cells, which was further used to kill the cancer cells. A synthetic Fab fragment of anti-HER2 antibody Fab37 with many Trp residues at hypervariable region was prepared and labeled with fluorescent dyes to obtain the UQ-bodies. The UQ-body could detect HER2 in solution at concentrations as low as 20 pM with an EC_{50} of 0.3 nM with a fourfold response. Fluorescence imaging of HER2-positive cells was successfully performed without any washing steps. To deliver small interfering RNA (siRNA) to cancer cells, a modified UQ-body with C-terminal 9R sequence was also prepared. HER2-positive cancer cells were effectively killed by polo-like kinase 1 siRNA intracellularly delivered by the UQ-body-9R. The novel approach employing siRNA-empowered UQ-body could detect and image the HER2 antigen easily and sensitively, and effectively kill the HER2-positive cancer cells.

KEYWORDS

antibody drug conjugate, cancer imaging, fluorescence quenching, high throughput screening, polo-like kinase

1 | INTRODUCTION

Antibodies are glycoproteins produced by the humoral immune system of vertebrates to protect individuals from damage from microorganisms, viruses, and toxins (Milstein, 1986). Antibodies have been amply studied concerning applications including immunoassays to detect materials in samples, diagnosis, and cancer therapy. Especially, combined with knowledge of biological mechanisms of various diseases, antibodies have been harnessed to target specific molecules on cells, which has proven valuable in the prevention and treatment of serious diseases, such as cancer (Ecker, Jones, & Levine, 2015; Leavy, 2010). An established target molecule is human epidermal growth factor receptor 2 (HER2), a receptor tyrosine kinase that normally controls the differentiation and proliferation of mammalian cells (Gutierrez & Schiff, 2011). HER2 is also frequently overexpressed in malignant cell populations, such as in the stomach and breast. HER2 has become an important biomarker for the

Jinhua Dong and Yuya Oka contributed equally to this study.

diagnosis and targeted therapy of breast cancer (Lavaud & Andre, 2014; Mendes et al., 2015). The specific binding of anti-HER2 antibody to HER2-positive cells can halt downstream signal transduction, which can result in the death of the cancer cells.

The Quenchbody (Q-body) immunoassay is a novel biosensing technology that employs fluorescence quenching of the appropriately conjugated dye by intrinsic tryptophan (Trp) residues in the variable region (Fv) of antibody. When the antigen is bound to the Q-body, the quenched dye is displaced from the protein and de-quenched, which results in increased fluorescence (Abe et al., 2011). Compared with conventional fluoroimmunoassays, the Q-body assay is simple and requires no additional reagents and steps to perform the detection. We have found that Q-body made of antibody Fab fragment (Ultra Q-body [UQ-body]) is more stable, and generally gives a higher antigen-dependent signal than the corresponding single-chain Fv-based Q-body. UQ-bodies have been successfully constructed for the detection of various substances, including small molecules, such as illegal drugs (Abe et al., 2014), pesticides (Zhao, Dong, Jeong, Okumura, & Ueda, 2018), and peptides, as well as large proteins, such as influenza virus hemagglutinin (Jeong, Dong, & Ueda, 2018) and the tight junction-associated membrane protein, claudin (Jeong et al., 2017). We have successfully imaged claudin-positive cancer cells by fluorescence microscopy without any washing steps, which could potentially be harnessed for use in cancer diagnostics.

The first goal of this study was to construct UQ-bodies for HER2. To detect HER2 with high sensitivity, an antibody with avid affinity and specificity is necessary. We chose Fab37, an anti-HER2 antibody fragment previously selected from a synthetic binary-encoded library by phage display. The most striking feature of this Fab fragment is its complementary determination regions (CDRs), most of which are encoded only Trp and serine (Ser) residues (Birtalan, Fisher, & Sidhu, 2010; Fisher et al., 2010; Figure 1a,b). When the dye is in close proximity, the Trp residues provide electrons to the fluorescent dye in its excited state by photoinduced electron transfer, which results in fluorescence quenching. Considering a large number of Trp residues (nine in V_H and five in V_L) and the high affinity for the HER2 extracellular domain (dissociation constant K_d: 0.44 nM), we decided to use this clone to prepare UQ-bodies.

RNA interference (RNAi) is a widely used technology to down-regulate the expression of specific cellular mRNA and has been exploited as a cancer therapy (Bumcrot, Manoharan, Koteliansky, & Sah, 2006; Mansoori, Sandoghchian Shotorbani, & Baradaran, 2014). Recently, several small interfering RNAs (siRNAs) were reported to induce cell death of both cancerous and normal cells. Therefore, target-specific siRNA delivery technology is considered critically important (Wu, Lopez-Berestein, Calin, & Sood, 2014). Among such attempts, Song et al. (2005) succeeded in the suppression of HIV-1 envelope gene by delivering siRNA with a fusion protein of anti-HIV-1 envelope Fab fragment and protamine. Protamine is an arginine (Arg)-rich nuclear protein that can replace histones late in the haploid phase of spermatogenesis and is believed to be essential for sperm head condensation and DNA stabilization (Balhorn, 2007). By employing the specific interaction between the polyarginine and the phosphates of nucleic acids, siRNA was successfully delivered into cells. As the second and more important goal of this study, we designed a UQ-body with a poly-Arg peptide to deliver functional siRNAs to explore its utility as an RNAi delivery agent for the efficient theranostics of HER2-positive cancer cells.

2 | MATERIALS AND METHODS

2.1 | Materials

Escherichia coli strains XL10-Gold (Stratagene, La Jolla, CA) was used for general cloning, SHuffle T7 express lysY (New England Biolabs, Ipswich, MA; Bessette, Aslund, Beckwith, & Georgiou, 1999; Levy, Weiss, Chen, Iverson, & Georgiou, 2001) was used for protein expression. Restriction and modification enzymes were purchased from Takara-Bio (Shiga, Japan), Toyobo Biochemicals (Osaka, Japan), Roche Diagnostics (Tokyo, Japan), or New England Biolabs. HER2 protein was obtained from Sino Biological (Beijing, China). 5(6)-TAMRA-C6-maleimide and ATTO520-maleimide were from AAT Bioquest (Sunnyvale, CA) and Atto-Tech (Siegen, Germany), respectively. A549 (CCL-185) and SK-BR3 (HTB30) cells were purchased from ATCC (Manassas, VA). Cell Light Endosome-RFP was purchased from Life Technologies (Tokyo, Japan). Fluorescein isothiocyanate (FITC)-conjugated AffiniPure $F(ab')_2$ Fragment Goat Anti-Human IgG + IgM (H + L) was purchased from Jackson Immuno Research Laboratories, Inc. Signal Silence PLK1 siRNA1 (#6292) and Control siRNA (Unconjugated, #6568) were purchased from Cell Signaling Technology Japan (Tokyo, Japan). Anti-PLK1 antibody (#36-298) was purchased from Abcam (Cambridge, UK). Monoclonal anti-β-tubulin antibody (#075K4875) was purchased from Sigma-Aldrich (St. Louis, MO). The variable region genes of anti-HER2 antibody Fab37 and other oligonucleotides were synthesized by Eurofins Genomics (Tokyo, Japan). Other chemicals, reagents, and antibodies, unless otherwise indicated, were obtained from Sigma or Wako Pure Chemicals (Osaka, Japan).

2.2 | Construction of plasmids

Previously, we constructed a vector pUQ1H-KTM219 to express Fab of anti-osteocalcin antibody KTM219 with a Cys tag at the H chain N terminus (Abe et al., 2014), and pUQ1L-MEM9 for the expression of Fab fragment against methamphetamine with a Cys tag at the L chain N-terminus. By changing the genes for both V_H and V_L in the above-mentioned vectors with the genes for Fab37, we constructed pUQH-Fab37 to express Fab37 with a Cys-tag (MAQIEVNCSNETG) at the H chain N-terminus (H-Fab37) and pUQL-Fab37 expresses Fab37 with a Cys-tag (MSKQIEVNCSNET) at the L chain N-terminus (L-Fab37; Figure 1c), respectively.

Briefly, to construct pUQH-Fab37, the V_H gene of Fab37 was digested from the plasmid encoding the *E. coli* codon-optimized synthetic gene for Fab37 with restriction endonucleases *Age*I and *Xho*I. pUQ1H-KTM219 was digested with same enzymes, purified and was ligated

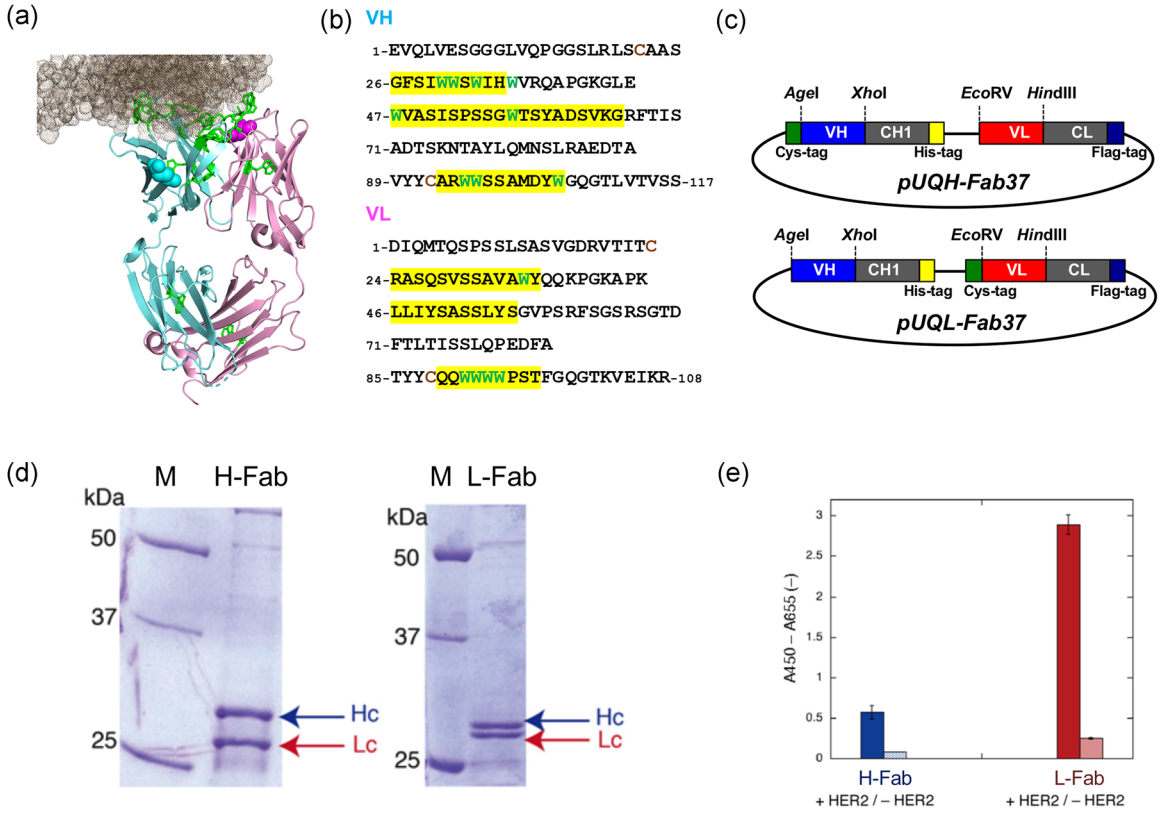

FIGURE 1 Structure and expression of Cys-tagged Fab37. (a) 3D structure of Fab37 complexed with HER2 (brown dots). Trp residues are shown in green. The N-terminal residues of H and L chains are shown in cyan and magenta balls, respectively. Drawn with Pymol based on PDB 3N85. (b) Amino acid sequence of Fab37 variable region. CDR residues based on IMGT (www.imgt.org) are marked in yellow. Trp (W) and Cys (C) residues are shown in green and brown, respectively. Sequences are numbered according to Kabat numbering scheme (Abhinandan & Martin, 2008). (c) Scheme of the experiment with the structures of expression vectors for Cys-tagged Fab37. (d) SDS-PAGE analysis of purified H-Fab and L-Fab proteins. The blue and red arrows show the heavy and light chains, respectively. (e) Antigen binding activity of H-Fab and L-Fab to recombinant HER2 immobilized by anti-DDDDK antibody. CDRs, complementary determination regions; HER2, human epidermal growth factor receptor 2; SDS-PAGE, sodium dodecyl sulfate-polyacrylamide gel electrophoresis; Trp, tryptophan [Color figure can be viewed at wileyonlinelibrary.com]

with *Age*I- and *Xho*I-digested V_H gene with Ligation High ver. 2 (Toyobo Biochemicals). *E. coli* XL10-Gold cells were transformed with the mixture and cultured on an LBA agar plate (1.0% tryptone, 0.5% yeast extract, 0.5% NaCl, 1.5% agar, 100 μg/ml ampicillin) at 37°C for overnight. The colonies containing targeted plasmid were screened by colony polymerase chain reaction (PCR) with primers T7promoter and T7terminator, and positive clones were cultivated for the preparation of plasmids. The sequences of the primers used in this study are shown in Table S1. The plasmid containing V_H gene of Fab37 was digested with *Eco*RV and *Hin*dIII to remove the V_L gene of KTM219 and inserted with V_L gene of Fab37 amplified with Fab37-VL-*Eco*RV and T7terminator, and digested with *Eco*RV and *Hin*dIII to construct resulting plasmid pUQH-Fab37.

Plasmid pUQL-Fab37 for the expression of L-Fab37 was constructed based on a previously constructed vector pUQ1L-MEM9. Briefly, the V_H and V_L genes of Fab37 were digested with *Age*I/*Xho*I and *Spe*I/*Hin*dIII, and serially cloned between the *Age*I/*Xho*I and *Spe*I/*Hin*dIII sites of pUQ1L-MEM9, respectively.

To construct pUQH-Fab37-9R, the gene encoding 9R peptide with *Eag*I sites on both sides was synthesized by PCR using two short oligonucleotides *Eag*I-9Arg back and *Eag*I-9Arg for. The amplified product was inserted to pUQH-Fab37 at *Eag*I site, which sits between Fd chain and His-Myc tag, using an In-Fusion HD cloning kit with cloning enhancer solution (Takara-Bio).

2.3 | Expression and purification of antibody fragments

E. coli SHuffle T7 express lysY cells were transformed with the plasmids and cultured on LBA agar plate at 30°C for overnight. Single colony was picked up and cultivated in LBA medium until OD_{600} became 0.5, when 0.4 mM isopropyl-thio-β-galactopyranoside was added to induce protein expression. The culture was continued for 16 hr while shaking at 200 rpm at 16°C. Intracellular soluble proteins were extracted using a One-shot cell disruptor (Constant Systems, Daventry, UK) and the Fabs purified

using Talon immobilized metal affinity resin according to the manufacturer's protocol (Clontech, Takara-Bio).

2.4 | Preparation of UQ-bodies

The purified Fabs were subjected to a Nanosep Centrifugal-3 k Ultrafiltration Device (Nihon Pall, Tokyo, Japan) and equilibrated with phosphate buffer (50 mM sodium phosphate, 100 mM NaCl, 10 mM EDTA, pH 7.4). A volume of immobilized Tris(2-carboxyethyl)phosphine hydrochloride disulfide reducing gel slurry (Thermo Fisher) equal to the volume of purified protein was added to a microtube and centrifuged at 50 × g for 1 min. After removing the supernatant, purified Fabs were added and incubated for 1 hr at room temperature on a rotating wheel. After centrifuging for 1 min, the supernatant was recovered and its concentration was determined using the Bradford assay (Bio-Rad, Tokyo, Japan) with bovine serum albumin (BSA) as a standard.

The reduced Fabs were labeled with TAMRA-C6-maleimide, or ATTO520-maleimide in the dark for 2 hr at 25°C. The molar ratio of protein to dye was one to ten. The product was subsequently incubated with 20 μl of Anti-DYKDDDDK tag antibody beads (Wako, Osaka, Japan). After incubation at room temperature for 2 hr, the beads were washed three times with wash buffer (20 mM phosphate, 0.5 M NaCl, 0.1% polyoxyethylene(23)lauryl ether, pH 7.4). The bound proteins were subsequently eluted with two 200 μl volumes of wash buffer containing 150 μg/ml of DYKDDDDK peptide. The purified UQ-bodies were then subjected to a Nanosep Centrifugal-3 k Ultrafiltration Device and equilibrated with PBST (0.05% Tween 20 in PBS).

2.5 | Analyses of UQ-bodies

To confirm the amount and purity of UQ-bodies, 10 μl each of the samples were separated by sodium dodecyl sulfate-polyacrylamide gel electrophoresis (SDS-PAGE). After electrophoresis, the gel was observed under a fluorescence imager Gel-Miére (Wako) to confirm the labeling of proteins followed by staining with a Quick-CBB staining kit (Wako). The mixture of Precision Plus Protein Unstained and Dual Color Standards (Bio-Rad) was used as molecular weight standards.

2.6 | Enzyme-linked immunosorbent assay

The antigen-binding activity of Fabs and UQ-bodies were tested by enzyme-linked immunosorbent assay (ELISA). The 96-well microplate (Greiner Bio-one, Tokyo, Japan) was coated overnight with 100 μl per well of anti-DDDDK-tag antibody (0.5 μg/ml, MBL, Nagoya, Japan) in PBS at 4°C. The plate was blocked at 25°C for 2 hr with 20% ImmunoBlock (DS Pharma Biomedical, Osaka, Japan), washed three times with PBST (0.05% Tween 20 in PBS), and incubated with 0.5 μg/ml of HER2(1-652) with C-terminal DDDDK tag (Sino Biological, Inc., Beijing, China) in PBS at 25°C for 1 hr. After washing, 100 μl/well of PBS containing 0 or 50 ng/ml of Fab was applied and incubated at 25°C for 1 hr. The plate was washed and incubated with 100 μl/well of 5000-fold diluted HRP/anti-His monoclonal conjugate (Wako) in PBS at 25°C for 1 hr. The plate was then washed three times with PBST again and developed with 100 μl/well TMBZ solution [100 μg/ml 3,3′,5,5′-tetramethylbenzidine (Sigma) and 0.04 μl/ml H_2O_2, in 100 mM NaOAc, pH 6.0]. After incubation for 5-30 min, the reaction was stopped by adding 50 μl/well of 10% sulfuric acid, and the absorbance was read using an SH-1000 microplate reader (Corona Electric, Ibaraki, Japan) at 450 nm with 655 nm as a control.

2.7 | Fluorescence spectroscopy

Purified UQ-body (12.5 ng, 1 nM) in 250 μl of PBST was added into a 5 mm × 5 mm quartz cell (Starna Scientific, Hainault, UK), and 2.5 μl of HER2 protein in PBST at variable concentration was added by titration. After each addition, the solution was incubated at 25°C for 5 min before the spectral measurements. As a control, quartz cells containing the same volume and amount of UQ-body were added by PBST instead of analyte solution. To evaluate the initial quenching of the Q-body, 250 μl of 7M guanidine hydrochloride, 100 mM dithiothreitol (DTT) was added instead of PBST to the cell. The fluorescence spectra were obtained at 25°C using a fluorescence spectrophotometer Model FP-8500 (Jasco, Tokyo, Japan) with excitation at 546 nm for TAMRA and 520 nm for ATTO520. The excitation and emission slit widths were set to 5.0 nm. Dose-response curves were fitted to a four-parameter logistic equation at the maximum emission wavelength, using Kaleida Graph 4.1 (Synergy Software, Reading, PA) and the EC_{50} value was calculated from the curve. The limit of detection was obtained as the estimated antigen concentration that shows the mean blank value plus 3 SD.

2.8 | Cellular imaging

U2OS, A549, and SK-BR3 cells were applied on a glass-based ø35 mm dish (Iwaki Technoglass, Tokyo, Japan) to 1×10^5 cells/well and cultured overnight with 5% CO_2 at 37°C in a humidified incubator. For conventional immunostaining, the cells were washed once with PBS, nonlabeled Fab37 was added at 0.5 ng/well and incubated on ice or at room temperature for 1 hr. After washing three times with PBS, secondary antibody, FITC-conjugated AffiniPure $F(ab')_2$ fragment goat anti-human IgG + IgM (H + L) at 0.15 μg/well was added and incubated for 1 hr. The cells were further washed with PBS three times and the fluorescence was observed on an EVOS FL cell imaging system with GFP/RFP filter cubes (Thermo Fisher Scientific). For imaging with UQ-body, overnight cultured cells were washed with PBS for three times and the UQ-body (ATTO-H UQ) in FACS buffer (PBS containing 1% BSA, 0.1% NaN_3) was added at 10 nM (0.5 μg/ml). After incubation on ice or at room temperature for 60-120 min, the fluorescence was observed. Cells were also costained with Cell Light Endosome–RFP (Thermo Fisher Scientific) at 2 μl/10^4 cells at the seeding of culture, to investigate the

localization of HER2-ATTO520 UQ-body complex. All the images were analyzed with the ImageJ software.

2.9 | RNA interference

A546 and SK-BR3 cells were seeded on ø6 cm dishes at 1×10^6 cells/dish and cultured overnight. Plk1 siRNA (final concentration of 10 nM) and ATTO-H UQ-9R protein (final 50 nM) in PBS were mixed and incubated for 30 min at room temperature, added to the culture medium and cultured for 48-72 hr. As control samples, cells with Plk1 siRNA only, with ATTO-H UQ and Plk1 siRNA, and with ATTO-H UQ-9R mixed with control siRNA were prepared and added. Two dishes for each sample were prepared, and one was treated with trypsin to count cell numbers to calculate the survival rate. Another dish was washed with PBS for three times and scraped with 100 µl of RIPA buffer (150 mM NaCl, 1% NP-40, 0.1% SDS, 1 mM phenylmethylsulfonylfluoride, 0.5% sodium deoxycholate, 1 mM sodium orthovanadate, pH7.4) to collect cells. The cells were disrupted by sonication for 15 s, and the lysate was collected by centrifuge at 15,000 rpm for 10 min, 4°C. The cell lysates thus prepared containing 40 and 25 µg of protein for A549 and SK-BR3, respectively, were separated by SDS-PAGE and transferred to a polyvinylidene fluoride membrane. After blocking with 1% skimmed milk in TBST (MTBST) for 1 hr at 25°C, the membrane was incubated with 1,000-fold diluted anti-Plk1 or anti-tubulin antibody in MTBST at 25°C for 1 hr, washed with TBST and incubated with 5,000-fold diluted HRP conjugated anti-mouse antibody at 25°C for 1 hr in MTBST. After washing three times with TBST, the chemiluminescent HRP substrate (WBKLS0100, Merck-Millipore) was added before imaging with a chemiluminescent imager Image Quant LAS 4010 (GE Healthcare, Tokyo, Japan).

3 | RESULTS

3.1 | Expression of Cys-tagged Fab37 in *E. coli*

To obtain highly responsive UQ-body, Fab37 fragments with N-terminal Cys tag for dye-labeling at the heavy or light chain were made using recombinant DNA technology and expression in *E. coli*, followed by labeling with the candidate dyes. For the expression of tagged Fab37, two expression vectors were constructed. In the pUQH-Fab37 vector for the expression of H-Fab, the gene encoding a Cys-tag (MAQIEVNCSNET) was added to the 5' end of V_H-C_H1(Fd)gene. In the pUQL-Fab37 vector for the expression of L-Fab, the gene for Cys-tag was added at the 5' end of L chain gene (Figure 1c). Construction of UQ-body with two Cys tags was not attempted considering the high content of Trp in the Fab37 fragment, because previous results showed that although higher quenching is achieved, double-labeled UQ-body sometimes shows lower sensitivity due to dye–dye interaction that competes with antigen binding (Abe et al., 2014).

E. coli SHuffle T7 Express lysY cells with oxidized cytoplasm were transformed with the aforementioned vectors, and used to express H-Fab and L-Fab. The expressed proteins were purified by immobilized metal affinity chromatography (IMAC) and further analyzed by SDS-PAGE. As shown in Figure 1d, two bands for Fd and light chain for both H-Fab and L-Fab were prominent. The molecular weights of the Fd and L chains estimated from the mobility on the gel appeared somewhat larger than the theoretical sizes of Fd and L chain in H-Fab (27.4 and 25.0 kDa, respectively) and in L-Fab (26.4 and 25.8 kDa, respectively). The reason for these discrepancies is unknown, but could possibly be related to their high contents of Ser and Trp. The antigen-binding activity of H-Fab and L-Fab was confirmed by ELISA using immobilized HER2 protein. As shown in Figure 1e, the two Fabs showed specific binding to the HER2 antigen. Although L-Fab displayed a stronger positive signal than H-Fab at the same apparent concentration, it also displayed a higher background signal without an immobilized antigen.

3.2 | Preparation of UQ-bodies

The UQ-body is an antibody Fab fragment that is specifically labeled with fluorescent dye(s) at the position(s) that enables antigen-dependent fluorescence emission. H-Fab and L-Fab proteins were labeled with TAMRA-C6-maleimide or ATTO520-maleimide to prepare the UQ-bodies. The structures for the abovementioned fluorescent dyes are shown in Figure 2a. Labeled antibody fragments were further purified with anti-DYKDDDDK antibody-coated beads. All the prepared UQ-bodies were separated by SDS-PAGE and the fluorescence of Fab fragments was observed using a fluorescence transilluminator.

Figure 2b shows the fluorescence of labeled H-Fab (H UQ-body) and L-Fab (L UQ-body) with TAMRA-C6-maleimide and ATTO520-maleimide, respectively. A fluorescent band corresponding to either the Fd of H UQ-body or the light chain of L UQ-body was clearly observed for each lane. The antigen-binding activity of TAMRA- and ATTO520-labeled UQ-bodies were also measured by ELISA with immobilized HER2 antigen (Figure S1a). The data clearly showed no major decrease in binding activity by the labeling.

3.3 | Denaturant- and antigen-dependent dequenching of UQ-bodies

In a single-labeled UQ-body, the fluorescence of the dye is considered to be quenched by the Trp residues in the variable region in its native structure. However, when the protein is denatured by denaturant, the quenching effect of Trp residues is significantly lowered due to the lower chance of collision between them. Therefore, the purified UQ-bodies were treated with 7M guanidine hydrochloride solution containing 100 mM DTT to evaluate the degree of quenching, which is a good parameter of its potential as a UQ-body (Abe et al., 2014). As shown in Figure 2c,e, the fluorescence intensity of TAM-H UQ-body and ATTO-H UQ-body increased up to 6.3- and 5.1-fold, respectively. On the other hand,

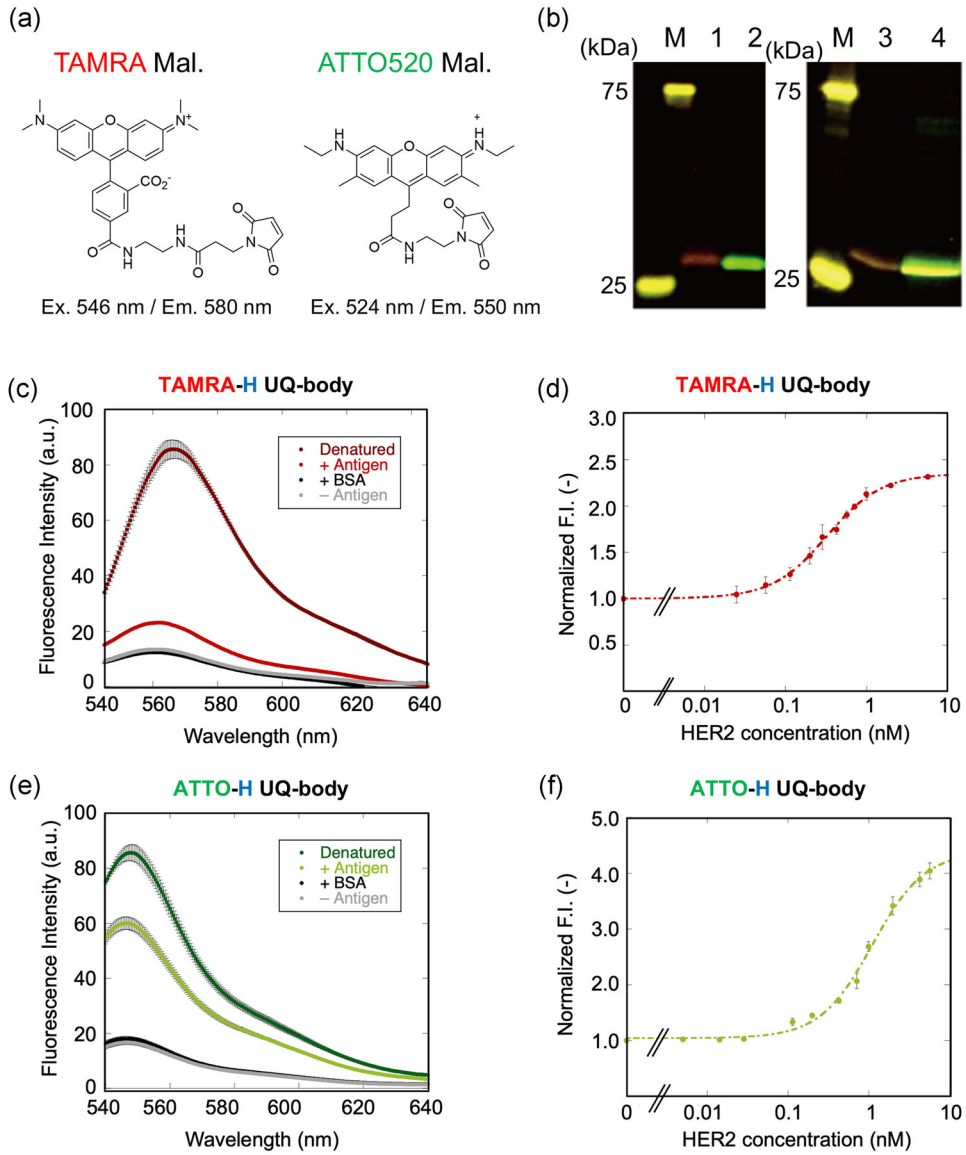

FIGURE 2 Preparation and analysis of UQ-bodies. (a) Structure of fluorescent dyes used for labeling H-Fab and L-Fab. (b) SDS-PAGE analysis of purified UQ-bodies. M: molecular weight markers showing two fluorescent bands at 25 and 75 kDa, 1: TAMRA-labeled H-Fab, 2: ATTO520-labeled H-Fab, 3: TAMRA-labeled L-Fab, 4: ATTO520-labeled L-Fab. (c and d) Fluorescence response of TAMRA-H UQ-body. Antigen- and denaturant-induced spectral change (c) and antigen dose-response based on the peak fluorescence (d). (e and f) The same for ATTO-H UQ-body. SDS-PAGE, sodium dodecyl sulfate-polyacrylamide gel electrophoresis; UQ-body, Ultra Quenchbody [Color figure can be viewed at wileyonlinelibrary.com]

that of TAM-L UQ-body and ATTO-L UQ-body increased up to 3.7- and 2.2-fold, respectively (Figure S2). When the antigen dependency of fluorescent response was evaluated using 0.7 nM HER2 and 1 nM UQ-body proteins, significant antigen-dependent responses were also observed. The antigen-dependent fluorescent responses for TAM-H and ATTO-H UQ-bodies were 1.7-and 3.6-fold, respectively. On the other hand, those for TAM-L and ATTO-L UQ-bodies were slightly lower values of 1.5-and 1.7-fold, respectively. However, the fluorescence did not change significantly when BSA was added as a negative control, especially for TAM-H and ATTO-H UQ-bodies. These results indicated higher and more specific responses of H-chain labeled UQ-bodies.

3.4 | Sensitive detection of HER2 protein in vitro

Based on the abovementioned results, Fab37-based TAM-H and ATTO-H UQ-bodies were used to quantify HER2 protein. As shown in Figure 2d,f, with the increased concentration of HER2, the fluorescence intensity of UQ-body was increased 2.3- and 4.0-fold above the background, for TAM-H and ATTO-H UQ-bodies, respectively. From the fitting of dose-response curves, the EC_{50} values of 3×10^{-10} M and 1.1×10^{-9} M were obtained for TAM-H and ATTO-H, respectively. The limit of detection for HER2 was 2.0×10^{-11} M for TAM-H and 8.0×10^{-11} M for ATTO-H UQ-bodies.

3.5 | One-step imaging of HER2-positive cancer cells

To examine the potential of UQ-body as a bioimaging reagent, one-step fluorescence imaging of HER2-positive cancer cells was attempted using ATTO-H UQ-body. Three human cancer cell lines —U2OS osteosarcoma, A549 lung carcinoma, and SK-BR3 breast adenocarcinoma—were used with different amounts of HER2 expression (Hassan et al., 2012). First, immunofluorescence imaging of the cells was performed according to the conventional procedure (Figure 3a). The staining pattern obtained with unconjugated H-Fab and FITC-labeled anti-human IgG + M after washing confirmed varied amounts of HER2 expression (U2OS < A549 < SK-BR3). On the other hand, after an incubation period of the cells with ATTO-H UQ-body for 1 hr, almost the same staining pattern was observed without the washing process (Figure 3b). It was demonstrated that one-step and specific detection of HER2 positive cells was successfully achieved using this UQ-body.

3.6 | Destruction of HER2-positive cancer cells by UQ-body mediated RNAi

When we observed the fluorescence images of A549 and SK-BR3 cells stained with ATTO-H UQ-body, a substantial portion of the fluorescence was observed inside the cells (Figure 3). When we costained the cells with the endosome marker, the fluorescence derived from the UQ-body closely colocalized with that from the marker (Figure S3). We reasoned that the UQ-body bound to cell surface HER2 was efficiently internalized by endocytosis, although 1% sodium azide was included in the fluorescence-activated cell sorting buffer. The observation also suggested the possibility that Fab37 could be used as an HER2-specific vehicle to deliver a cytotoxic drug or reagent, such as siRNA, to kill HER2-positive malignant cells. With the aim of endowing the UQ-body with cancer-killing activity, we attempted to use this UQ-body as a vehicle to deliver siRNA by appending a consecutive nine arginine (9R) sequence to its C-terminal region (Zhang et al., 2014; Figure 4).

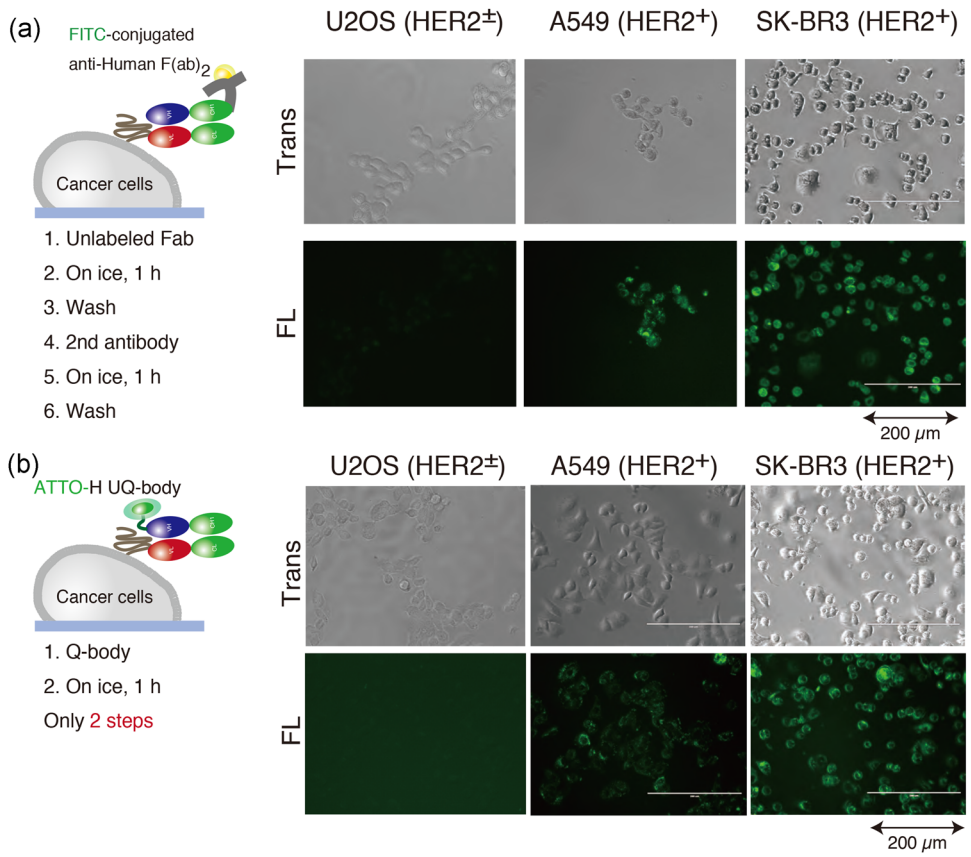

FIGURE 3 Wash-free fluorescence imaging of cancer cells with ATTO-H UQ-body. Observation of cancer cells with varied amounts of HER2 expression using the UQ-body. (a) Conventional immunostaining with H-Fab and FITC-labeled secondary antibody. (b) One-step staining with ATTO-H UQ-body. FITC, fluorescein isothiocyanate; HER2, human epidermal growth factor receptor 2; UQ-body, Ultra Quenchbody [Color figure can be viewed at wileyonlinelibrary.com]

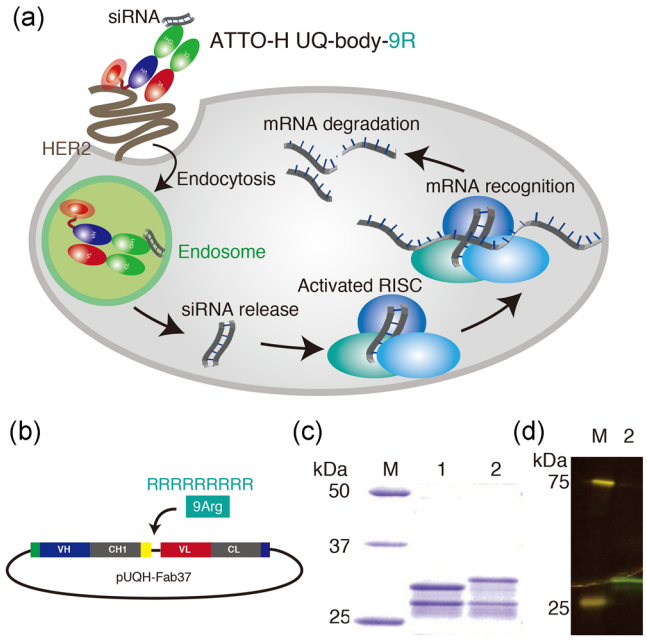

FIGURE 4 Intracellular delivery of siRNA by UQ-body-9R. (a) Schematic image of the delivery process. The UQ-body made of H-Fab-9R carrying siRNA binds to HER2 and delivers siRNA into HER2-positive cells. The released siRNA binds to RISC and results in RNAi. (b) Scheme of the vector for the expression of H-Fab-9R. (c) Expression and purification of H-Fab (Lane 1) and H-Fab-9R (Lane 2). (d) Fluorescence image of ATTO-H Fab-9R labeled with ATTO520 (Lane 2). M: molecular weight markers. HER2, human epidermal growth factor receptor 2; RISC, RNA-induced silencing complex; RNAi, RNA interference; siRNA, small interfering RNA; UQ-body, Ultra Quenchbody [Color figure can be viewed at wileyonlinelibrary.com]

For the efficient killing of malignant cells by siRNA, polo-like kinase 1 (Plk1) was chosen as the target protein. Plk1 belongs to the Plk family of kinases whose depletion causes abnormal segregation of chromatin DNA (Cheng, Lowe, Sinclair, Nigg, & Johnson, 2003; Lowery, Lim, & Yaffe, 2005; Strebhardt, 2010). As shown in Figure 4a, UQ-body made of H-Fab-9R is expected to bind to siRNA through the 9R guanidine group cluster as well as to HER2 at the Fab region. The 9R-tagged UQ-body will be delivered into cells by endocytosis and release siRNA in the acidic environment of the endosome. The released siRNA will be transported to cytosol, where it is incorporated into the RNA-induced silencing complex (RISC), which is then activated to recognize and degrade mRNA. RISC will recognize mRNAs and degrade them. This will halt translation and cause the death of the cancer cells.

3.7 | Efficient delivery of Plk1 siRNA by UQ-body-9R

For the expression of Fab37 appended with the 9R sequence, the pUQH-Fab37-9R expression vector (Figure 4b) was constructed. The protein was successfully expressed using *E. coli* SHuffle T7 lysY, purified by IMAC, and analyzed by SDS-PAGE. As shown in Figure 4c, two clear bands stand for Fd and light chain were observed (lane 2). The band positions roughly matched the molecular weights calculated for Fd and L chain in H-Fab37-9R (29.0 kDa and 25.0 kDa, respectively). The UQ-body was prepared with the same protocol as previously described and fluorescence of ATTO-H UQ-body-9R was also observed (Figure 4d). The antigen-binding activity was also evaluated by ELISA, and both unlabeled and labeled H-Fab37-9R were found to retain specific antigen-binding activity to immobilized HER2 protein (Figure S1b).

When we costained HER2-positive A549 and SK-BR3 cells with ATTO-H UQ-9R and the endosome marker, the fluorescence derived from the UQ-body closely colocalized with it, as in the case of ATTO-H UQ-body (Figure S4). Hence, the 9R sequence did not affect the UQ-body's activities of antigen-dependent fluorescence activation as well as the endosomal uptake.

We then tested the ability of this modified UQ-body as the delivery reagent of siRNA. A549 and SK-BR3 cells were treated with Plk1 siRNA alone, UQ-body and Plk1 siRNA, UQ-body-9R and unrelated siRNA, and UQ-body-9R and Plk1 siRNA, and analyzed with nontreated cells as a control. Figure 5a shows the result of western blot analysis after 72-hr incubation at 37°C. ATTO-H UQ-body-9R and Plk1 siRNA-treated A549 cells displayed lower expression of Plk1 than the other four samples that showed similar expression levels. In SK-BR3 cells, similar results were observed. In both experiments, β-tubulin was included as a standard control.

To evaluate the cytotoxic effect of Plk1 downregulation, cell numbers after 72-hr incubation with the same reagents were counted (Figure 5b). In the case of A549 cells, compared with the other four samples, when treated with ATTO-H UQ-body-9R and Plk1 siRNA, the viable cell number decreased to 35% of the control cells without treatment. In the case of SK-BR3 cells, only 20% of the cells survived in the same condition. The cells with other treatments did not show significant drop in cell number. These results clearly demonstrated that the HER2 UQ-body with 9 × Arg sequence efficiently delivered Plk1 siRNA into cells and induced RNAi to suppress Plk1 expression, which resulted in depletion of the HER2 positive cancer cells.

4 | DISCUSSION

The presently described Q-body technology is a relatively new homogenous immunoassay approach. It affords simpler and faster detection than previous heterogeneous immunoassays, such as ELISA and immunofluorescence, yet with sufficient sensitivity and selectivity. Although Q-bodies specific to small molecules (peptides and haptens) were relatively well characterized, successful detection of proteins including serum albumin and claudin 4 have been reported (Jeong et al., 2017). Especially, Fab-based, double-labeled UQ-bodies showed higher responses than scFv -based, single-labeled Q-bodies, and double-labeled UQ-bodies were successfully used to image overexpressed claudin 4 on LoVo colon cancer cells by wash-free fluorescence imaging. However, the detection limit attained therein was several nM, which was similar to the dissociation constant of the original antibody. In this study, we developed novel

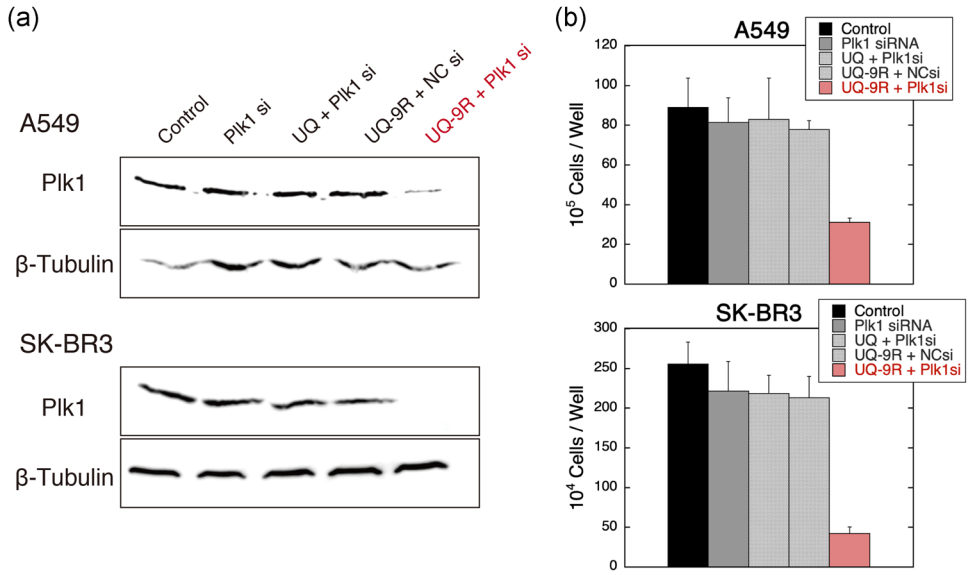

FIGURE 5 Efficient delivery of Plk1 siRNA and killing of HER2-positive cancer cells by UQ-body-9R. (a) The amounts of Plk1 protein in A549 and SK-BR3 cells detected by western blot analysis, after the 72-hr treatments. (b) Enumeration of viable cells after combination treatment with UQ-body-9R (UQ-9R) and Plk1 siRNA (red) with its controls. Error bars show 1 SD of three samples. HER2, human epidermal growth factor receptor 2; siRNA, small interfering RNA; UQ-body, Ultra Quenchbody [Color figure can be viewed at wileyonlinelibrary.com]

UQ-bodies with high Trp content to detect HER2, a very important cancer diagnostic/therapeutic marker protein (Gutierrez & Schiff, 2011; Haneef et al., 2014). HER2 could be detected with a limit of detection in the 20 pM range, which is one magnitude lower than the K_d of original Fab37 (0.44 nM).

According to previous analyses (Abe et al., 2011; Ohashi et al., 2016), the quenching of a single dye incorporated into Q-bodies is considered to occur solely by the Trp residues in its variable region through a photo-induced electron transfer mechanism (Abe et al., 2011; Buschmann, Weston, & Sauer, 2003; Marme, Knemeyer, Sauer, & Wolfrum, 2003; Vaiana et al., 2003). According to the amino acid sequences, the variable region of Fab37 harbors nine Trp residues in Fd and five residues in the L chain. Some of these Trp residues directly or indirectly interact with the fluorescent dye, and provide electrons to the excited dye, resulting in the transition of the molecule back to the ground state without emitting fluorescence. This time, the higher antigen-dependent dequenching achieved by H UQ-bodies might be due to the higher Trp contents and more specific antigen recognition by H chain CDRs, since they are closer to H-chain N-terminus (Figure 1a). On the contrary, less antigen-specific dequenching observed for L UQ-bodies (Figure S2) might indicate less specific antigen recognition of Trp residues in V_L CDRs, which are closer to L-chain N-terminus. Also, compared with TAM-H UQ-body, fourfold higher EC_{50} value was obtained for ATTO-H UQ-body. Although the precise reason is yet to be clarified, Q-bodies with higher degree of quenching tend to show increased EC_{50} values. Probably, this is due to the stronger interaction of ATTO520 dye and the Trp-containing binding site of this antibody, which competes with antigen binding. We believe that the selection of such a Trp-rich V region from a synthetic phage library, as in the case of Fab37, will be a very promising way to obtain UQ -bodies with high quenching/dequenching behavior.

Our results also showed the potential of UQ-bodies as a potent tool for in situ cancer diagnosis. Biological imaging of live cells is a challenging and troublesome task for biotechnologists and analytical chemists, since at least one washing step is necessary to remove background fluorescence signal. In this study, we demonstrated that UQ-bodies could be used to stain cancer cells without any washing steps. In our previous study (Jeong et al., 2017), by using UQ-bodies that show 2.5-3-fold antigen-dependent dequenching response, we have successfully imaged claudin-positive cancer cells without any washing steps. When we performed the same assay using randomly AF488-labeled UQ-body, no clear cellular image was observed with high background fluorescence. Hence, the fourfold response achieved this time is considered necessary and also enough to achieve fluorogenic wash-free imaging. All these results suggest the utility of the UQ-body as a handy tool to study the process of cancer cells and for the diagnosis of HER2-positive disease. Furthermore, with blue light irradiation, it could become a real-time imaging tool to visualize cancer cells with low background, helping surgeons to completely dissect cancer cells from their patients.

Lastly, another remarkable result we reached in this study is that UQ-bodies tethered with siRNA could be used not only as a fluorogenic imaging probe but also as an effective therapeutic to kill target malignant cell populations. By the fusion of an Arg-rich sequence, therapeutic siRNA can be delivered into the cytoplasm of cancer cells, inducing their death by suppressing the target protein expression. The UQ-body described in this study could be an ideal tool for theranostics of serious diseases, especially cancer.

ACKNOWLEDGMENTS

We deeply thank Tatsuya Niwa and Hideki Taguchi for their help of western blot analysis, and the Division of Biomaterial Analysis, Technical

Department, Tokyo Institute of Technology for nucleic acid sequence analysis. This study was partly supported by the JSPS KAKENHI (Grant Numbers JP15H04191, JP18H03851, and JP26420793) from the Japan Society for the Promotion of Science, Japan, by Dynamic Alliance for Open Innovation Bridging Human, Environment and Materials from MEXT, Japan, by the National Natural Science Foundation of China (Grant Number: 21775064) and Shandong Provincial Natural Science Foundation (Grant Number: ZR2017MB037), and by the Hongik University new faculty research support fund.

CONFLICT OF INTERESTS

The authors declare that there are no conflict of interests.

ORCID

Jinhua Dong http://orcid.org/0000-0002-7417-1932
Hiroshi Ueda http://orcid.org/0000-0001-8849-4217

REFERENCES

Abe, R., Jeong, H. J., Arakawa, D., Dong, J., Ohashi, H., Kaigome, R., … Ueda, H. (2014). Ultra Q-bodies: Quench-based antibody probes that utilize dye-dye interactions with enhanced antigen-dependent fluorescence. *Scientific Reports*, *4*, 4640. https://doi.org/10.1038/srep04640

Abe, R., Ohashi, H., Iijima, I., Ihara, M., Takagi, H., Hohsaka, T., & Ueda, H. (2011). "Quenchbodies": Quench-based antibody probes that show antigen-dependent fluorescence. *Journal of the American Chemical Society*, *133*(43), 17386–17394. https://doi.org/10.1021/ja205925j

Abhinandan, K. R., & Martin, A. C. (2008). Analysis and improvements to Kabat and structurally correct numbering of antibody variable domains. *Molecular Immunology*, *45*(14), 3832–3839. https://doi.org/10.1016/j.molimm.2008.05.022

Balhorn, R. (2007). The protamine family of sperm nuclear proteins. *Genome Biology*, *8*(9), 227. https://doi.org/10.1186/gb-2007-8-9-227

Bessette, P. H., Aslund, F., Beckwith, J., & Georgiou, G. (1999). Efficient folding of proteins with multiple disulfide bonds in the *Escherichia coli* cytoplasm. *Proceedings of the National Academy of Sciences of the United States of America*, *96*(24), 13703–13708.

Birtalan, S., Fisher, R. D., & Sidhu, S. S. (2010). The functional capacity of the natural amino acids for molecular recognition. *Molecular BioSystems*, *6*(7), 1186–1194. https://doi.org/10.1039/b927393j

Bumcrot, D., Manoharan, M., Koteliansky, V., & Sah, D. W. (2006). RNAi therapeutics: A potential new class of pharmaceutical drugs. *Nature Chemical Biology*, *2*(12), 711–719. https://doi.org/10.1038/nchembio839

Buschmann, V., Weston, K. D., & Sauer, M. (2003). Spectroscopic study and evaluation of red-absorbing fluorescent dyes. *Bioconjugate Chemistry*, *14*(1), 195–204. https://doi.org/10.1021/bc025600x

Cheng, K. Y., Lowe, E. D., Sinclair, J., Nigg, E. A., & Johnson, L. N. (2003). The crystal structure of the human polo-like kinase-1 polo box domain and its phospho-peptide complex. *EMBO Journal*, *22*(21), 5757–5768. https://doi.org/10.1093/emboj/cdg558

Ecker, D. M., Jones, S. D., & Levine, H. L. (2015). The therapeutic monoclonal antibody market. *mAbs*, *7*(1), 9–14. https://doi.org/10.4161/19420862.2015.989042

Fisher, R. D., Ultsch, M., Lingel, A., Schaefer, G., Shao, L., Birtalan, S., … Eigenbrot, C. (2010). Structure of the complex between HER2 and an antibody paratope formed by side chains from tryptophan and serine. *Journal of Molecular Biology*, *402*(1), 217–229. https://doi.org/10.1016/j.jmb.2010.07.027

Gutierrez, C., & Schiff, R. (2011). HER2: Biology, detection, and clinical implications. *Archives of Pathology and Laboratory Medicine*, *135*(1), 55–62. https://doi.org/10.1043/2010-0454-RAR.1

Haneef, K., Naeem, N., Khan, I., Iqbal, H., Kabir, N., Jamall, S., … Salim, A. (2014). Conditioned medium enhances the fusion capability of rat bone marrow mesenchymal stem cells and cardiomyocytes. *Molecular Biology Reports*, *41*(5), 3099–3112. https://doi.org/10.1007/s11033-014-3170-1

Hassan, S. E., Bekarev, M., Kim, M. Y., Lin, J., Piperdi, S., Gorlick, R., & Geller, D. S. (2012). Cell surface receptor expression patterns in osteosarcoma. *Cancer*, *118*(3), 740–749. https://doi.org/10.1002/cncr.26339

Jeong, H.-J., Dong, J., & Ueda, H. (2018). Single-step detection of the influenza virus hemagglutinin using bacterially-produced Quenchbodies. *Sensors*, *19*(1), 52. https://doi.org/10.3390/s19010052

Jeong, H. J., Kawamura, T., Iida, M., Kawahigashi, Y., Takigawa, M., Ohmuro-Matsuyama, Y., … Ueda, H. (2017). Development of a Quenchbody for the detection and imaging of the cancer-related tight-junction-associated membrane protein claudin. *Analytical Chemistry*, *89*(20), 10783–10789. https://doi.org/10.1021/acs.analchem.7b02047

Lavaud, P., & Andre, F. (2014). Strategies to overcome trastuzumab resistance in HER2-overexpressing breast cancers: Focus on new data from clinical trials. *BMC Medicine*, *12*, 132. https://doi.org/10.1186/s12916-014-0132-3

Leavy, O. (2010). Therapeutic antibodies: Past, present and future *Nature Reviews Immunology*, *10*(5), 297. https://doi.org/10.1038/nri2763

Levy, R., Weiss, R., Chen, G., Iverson, B. L., & Georgiou, G. (2001). Production of correctly folded Fab antibody fragment in the cytoplasm of *Escherichia coli* trxB gor mutants via the coexpression of molecular chaperones. *Protein Expression and Purification*, *23*(2), 338–347. https://doi.org/10.1006/prep.2001.1520

Lowery, D. M., Lim, D., & Yaffe, M. B. (2005). Structure and function of polo-like kinases. *Oncogene*, *24*(2), 248–259. https://doi.org/10.1038/sj.onc.1208280

Mansoori, B., Sandoghchian Shotorbani, S., & Baradaran, B. (2014). RNA interference and its role in cancer therapy. *Advanced Pharmaceutical Bulletin*, *4*(4), 313–321. https://doi.org/10.5681/apb.2014.046

Marme, N., Knemeyer, J. P., Sauer, M., & Wolfrum, J. (2003). Inter- and intramolecular fluorescence quenching of organic dyes by tryptophan. *Bioconjugate Chemistry*, *14*(6), 1133–1139. https://doi.org/10.1021/bc0341324

Mendes, D., Alves, C., Afonso, N., Cardoso, F., Passos-Coelho, J. L., Costa, L., … Batel-Marques, F. (2015). The benefit of HER2-targeted therapies on overall survival of patients with metastatic HER2-positive breast cancer—a systematic review. *Breast Cancer Research*, *17*, 140. https://doi.org/10.1186/s13058-015-0648-2

Milstein, C. (1986). From antibody structure to immunological diversification of immune response. *Science*, *231*(4743), 1261–1268.

Ohashi, H., Matsumoto, T., Jeong, H. J., Dong, J., Abe, R., & Ueda, H. (2016). Insight into the working mechanism of Quenchbody: Transition of the dye around antibody variable region that fluoresces upon antigen binding. *Bioconjugate Chemistry*, *27*(10), 2248–2253. https://doi.org/10.1021/acs.bioconjchem.6b00217

Song, E., Zhu, P., Lee, S. K., Chowdhury, D., Kussman, S., Dykxhoorn, D. M., … Lieberman, J. (2005). Antibody mediated in vivo delivery of small interfering RNAs via cell-surface receptors. *Nature Biotechnology*, *23*(6), 709–717. https://doi.org/10.1038/nbt1101

Strebhardt, K. (2010). Multifaceted polo-like kinases: Drug targets and antitargets for cancer therapy. *Nature Reviews. Drug Discovery*, *9*(8), 643–660. https://doi.org/10.1038/nrd3184

Vaiana, A. C., Neuweiler, H., Schulz, A., Wolfrum, J., Sauer, M., & Smith, J. C. (2003). Fluorescence quenching of dyes by tryptophan: Interactions at atomic detail from combination of experiment and computer simulation. *Journal of the American Chemical Society*, *125*(47), 14564–14572. https://doi.org/10.1021/ja036082j

Wu, S. Y., Lopez-Berestein, G., Calin, G. A., & Sood, A. K. (2014). RNAi therapies: Drugging the undruggable. *Science Translational Medicine*, *6*(240), 240ps7. https://doi.org/10.1126/scitranslmed.3008362

Zhang, X., Xie, J., Sun, Y., Xu, H., Du, T., Liu, Z., … Xiao, Y. (2014). High-level expression, purification, and characterization of bifunctional ScFv-9R fusion protein. *Applied Microbiology and Biotechnology*, *98*(12), 5499–5506. https://doi.org/10.1007/s00253-014-5541-x

Zhao, S., Dong, J., Jeong, H.-J., Okumura, K., & Ueda, H. (2018). Rapid detection of the neonicotinoid insecticide imidacloprid using a quenchbody assay. *Analytical and Bioanalytical Chemistry*, *410*, 4219–4226. https://doi.org/10.1007/s00216-018-1074-y

SUPPORTING INFORMATION

Additional supporting information may be found online in the Supporting Information section.

How to cite this article: Dong J, Oka Y, Jeong H-J, Ohmuro-Matsuyama Y, Ueda H. Detection and destruction of HER2-positive cancer cells by Ultra Quenchbody-siRNA complex. *Biotechnology and Bioengineering*. 2020;117:1259–1269. https://doi.org/10.1002/bit.27302